International Journal of Theoretical Physics (2026) 65:212
https://doi.org/10.1007/s10773-026-06395-1

RESEARCH

Bifurcation Analysis, Stability, and Unravelling Soliton Solutions of the Cubic-Quintic Nonlinear Model in Superconductivity for Steady Ion-Cyclotron Waves

Md. Mamunur Roshid[1] · Ramy M. Hafez[2] · Yakup Yildirim[3,4] · Wen-Xiu Ma[5,6,7,8]

Received: 14 April 2026 / Accepted: 22 June 2026

Abstract
This work studies the dynamical behaviors of the generalized nonlinear evolution equation (GNLEE) introduced by Chen (2003), which is significant in explaining superconductivity in steady ion-cyclotron waves in nonhomogeneous plasma and drift cyclotron waves. This study investigates the model's dynamic properties using both analytical and numerical methods, with a focus on bifurcation analysis. First, wave transformation is used to convert the model into its standard form. This approach helps predict the creation or disappearance of equilibrium arguments, limit cycles, and soliton structures. The system's dynamic behavior is then analyzed using phase and Hamiltonian portraits for different parameter values. Furthermore, we identify dark-type bell-wave, bright periodic, kink, bright-type, anti-kink, and solitary-wave solutions by manipulating parameters, using their Hamiltonians, and integrating heteroclinic and homoclinic orbits. The visual representation of these characteristics is achieved by carefully selecting the appropriate parameters. Finally, the MI also studies the proposed model to explain how small changes in field amplitude give rise to solitary structures, domain walls, and vortices. MI study of the Landau–Ginsburg–Higgs model shows how nonlinear interactions influence wave evolution and establish stability constraints in optical, quantum, and cosmic environments. From the above analysis, the applied method is more effective at capturing complex phenomena.

Keywords Bifurcation analysis · Soliton solution · Modulation instability · Steady ion-cyclotron waves · Generalized nonlinear evolution equation

1 Introduction

Nonlinear mathematical equations play a pivotal role in exploring the complex behaviors of various processes that cannot be adequately described by linear models. Its importance derives from the ability to replicate real-world systems defined by nonlinear interactions, feedback mechanisms, and energy transfers. It addresses the transmission of waves in fluids, plasmas, optical fibers, and Bose–Einstein condensates, enabling accurate forecasts of turbulence, rogue waves, and energy localization. In applied sciences, it facilitates the

Extended author information available on the last page of the article development of sophisticated communication systems, the optimization of nonlinear optical devices, and the analysis of vibration patterns in materials.

In 2003, Chen [10] presented novel generalized nonlinear evolution equations featuring dual power nonlinearity to investigate soliton solutions as follows:

$$L_{tt} + aL_{ss} + bL + cL^q + pL^{2q-1} = 0 \tag{1}$$

Here a, p, b, c and $q \neq 1 > 0$ are non-zero parameters. This model comprises significant nonlinear equations frequently employed in mathematical physics and engineering. Depend on the parameters a, b, c, p, and q, Eq. (1) represents many significant nonlinear models. In 2021, Bai [11] established a new form of the model Eq. (1) by setting $p = 0, q = 3$ in the subsequent form:

$$L_{tt} + aL_{ss} + bL + cL^3 = 0 \tag{2}$$

For$a = -1, b = -\alpha^2, c = h^2, p = 0$, and $q = 3$, Eq. (1) converts the differential equation known as the Landau–Ginzburg–Higgs (LGH) equation into the subsequent form:

$$L_{tt} - L_{ss} - \alpha^2 L + h^2 L^3 = 0 \tag{3}$$

Here α, h are real parameters, and the ion-cyclotron wave function is $L = L(s, t)$. This model was introduced by the mathematician Landau, and Ginzburg elucidated superconductivity in relation to steady ion-cyclotron waves in nonhomogeneous plasma and drift cyclotron waves [12], Additionally, the nonlinear model represented by Eq. (3) encompasses the Duffing equation, the Klein-Gordon, the Phi-4, and the Sine–Gordon [13–15] equations, which are contingent upon the constants a, b, c. Many scientists studied the LGH model using diverse analytical methods such as ansatz technique [16], (G´/G, 1/G)-expansion [17], first integral [18], NMSE [19], exponential function [20], generalized Kudryashov [21], and extended tanh [22], variational iteration [23] methods, and so on. In this research work, we introduced a new generalized form of the NLEE in Eq. (1) for the case $q = 3$ which has the following form:

$$L_{tt} + aL_{xx} + bL + cL^3 + pL^5 = 0 \tag{4}$$

This equation is particularly significant for describing complex phenomena in the fields of Engineering and mathematical physics.

Bifurcation analysis [24–26] is crucial for understanding the dynamics of nonlinear systems, particularly with respect to parameter variations. In contrast to linear systems, nonlinear systems may undergo substantial changes in dynamics with minimal modifications. Bifurcation analysis proficiently delineates transitions, including shifts from stable to unstable states, oscillatory patterns, or chaotic dynamics. It is essential for forecasting unforeseen results in biological, technical, or physical domains. Researchers have used bifurcation theory to generate diverse waveforms, including bell-type, solitary, periodic, and kink-type waves, in numerous nonlinear Schrödinger models, employing dynamical systems methods. Targeted efforts have yielded traveling wave solutions via phase portrait analysis and Hamiltonian energy levels in NLSE-type models [27, 28]. They also employed phase-plane techniques for its parametrization, resulting in wave patterns that encompass solitary, kink, breaking, and various elliptic or trigonometric forms.

Most of the researchers studied the planar dynamics system and orbit-wise wave propagation through bifurcation theory that should follow an ordinary differential model in [27, 28] and has a subsequent dynamical system for as:

$$\begin{cases} \frac{d\mathcal{U}}{d\psi} = Y \\ \frac{dy}{d\psi} = -\frac{p_2}{p_1}U - \frac{p_3}{p_1}\mathcal{U}^3 \end{cases} \tag{5}$$

The Hamiltonian form of the system is $H(N, R) = \frac{R^2}{2} - \left(-\frac{\frac{p_2}{p_1}\mathcal{U}^2}{2} - \frac{\frac{p_3}{p_4}\mathcal{U}^4}{4}\right)$. In this research we try to study the planar dynamics [29, 30] with a cubic-quintic term as:

$$\begin{cases} \frac{d\mathfrak{U}}{d\Xi} = L \\ \frac{d\mathfrak{U}}{d\Xi} = \frac{1}{\mathfrak{I}_1}\left(-\mathfrak{I}_2\mathfrak{U} - \mathfrak{I}_3\,\mathfrak{U}^3 - \mathfrak{I}_4\,\mathfrak{U}^5\right) \end{cases} \tag{6}$$

According to the author, although the GNLEEs in Eq. (2) have been well studied, the model's contributions remain inadequate. The research we conducted has several limitations. It is clear that this equation requires more investigation using bifurcation theory. The primary goal of the suggested theory is to amplify the free parametric terms of the Hamiltonian system. Motivated by previous studies, we relax the constraints on current parameters to obtain wave solutions. Here, bifurcation theory is used to develop the wave solutions for the GNLEEs. The aforementioned contributions make it evident that the various symmetry point classes will pose substantial problems. By integrating along the homoclinic or heteroclinic orbits, we can ascertain the wave solutions (Table 1) (Figs. 1, 2, 3 and 4).

2 Bifurcation Breakdown

Now we consider a wave transformation as:

$$L(s,\ t) = \mathfrak{U}(\Xi);\ \Xi = mx - nt \tag{7}$$

By substituting Eq. (5) into Eq. (4), we obtain,

$$\left(\Updownarrow^2 - a\backslash^2\right)\mathfrak{U}'' + b\mathfrak{U} + c\mathfrak{U}^3 + p\mathfrak{U}^5 = 0 \tag{8}$$

Equation (6) becomes:

$$\mathfrak{U}'' = -\frac{\left(b\mathfrak{U} + c\mathfrak{U}^3 + p\mathfrak{U}^5\right)}{\left(m^2 - n^2\right)} \tag{9}$$

According to the transformation of Galilean, Eq. (7) has the subsequent form:

$$\begin{cases} \frac{d\mathfrak{U}}{d\Xi} = L \\ \frac{d\mathcal{L}}{d\Xi} = \frac{1}{\mathfrak{I}_1}\left(-\mathfrak{I}_2\mathfrak{U} - \mathfrak{I}_3\mathfrak{U}^3 - \mathfrak{I}_4\mathfrak{U}^5\right) \end{cases} \tag{10}$$

Here $\mathfrak{I}_1 = \left(m^2 - n^2\right), \mathfrak{I}_2 = b, \mathfrak{I}_3 = c, \mathfrak{I}_4 = p.$
For the system (8), the Hamiltonian structure is:

$$\mathbb{H}(\mathfrak{U}, \mathcal{L}) = \frac{1}{\mathfrak{I}_1}\left(\frac{\mathfrak{I}_2\mathfrak{U}^2}{2} + \frac{\mathfrak{I}_4\mathfrak{U}^6}{6} + \frac{\mathfrak{I}_3\mathfrak{U}^4}{4}\right) + \frac{\mathcal{L}^2}{2} = h$$

Table 1 Explanation of the dynamical behaviors and equilibrium points

Parametric Condition/Event		Equilibrium points (EP)	Behavior of equilibrium points (EP) and phase portrait		Behaviors of system (10)
$\mathfrak{J}_3^2 \geq 4\mathfrak{J}_2\mathfrak{J}_4$(or $\mathfrak{J}_3^2 < 4\mathfrak{J}_2\mathfrak{J}_4$), $\mathfrak{J}_3\mathfrak{J}_4 > 0$	$\frac{\mathfrak{J}_2}{\mathfrak{J}_1} > 0$	$N_0(0,0)$	The EP is the saddle point seen in Fig. 1i		Unstable
	$\frac{\mathfrak{J}_2}{\mathfrak{J}_1} < 0$	$N_0(0,0)$,	The EP is the saddle point seen in Fig. 1(ii)		Stable
$\mathfrak{J}_3^2 = 4\mathfrak{J}_1\mathfrak{J}_4$ or $\mathfrak{J}_3\mathfrak{J}_4 < 0$	$-\frac{\mathfrak{J}_2}{\mathfrak{J}} < 0$	$N_0(0,0)$, $N_1(r_1,0)$, $N_2\left(r_2,0\right)$;$r_{1,2} = \pm\sqrt{-\frac{\mathfrak{J}_3}{2\mathfrak{J}_4}}$	Since $D_{0,0} < 0, D_{1,0} = D_{2,0} = 0$, The EP N_0 is the saddle point and $N_{1,2}$ are cups point seen in Fig. 2i		Unstable at N_0, N_1,and N_2
	$-\frac{\mathfrak{J}_2}{\mathfrak{J}_1} > 0$	$N_0(0,0)$, $N_1(r_1,0)$,$N_2\left(r_2,0\right)$;	Since $D_{0,0} > 0, Trace\left(M\left(N_{1,2}\right)\right) = 0$,$D_{1,0} = D_{2,0} = 0$, the EP N_0 is the Centre point and $N_{1,2}$ are cups point seen in Fig. 2(ii)		Stable at N_2 N_0, and Unstable at N_1 ,and
$\mathfrak{J}_2\mathfrak{J}_4 < 0$	$-\frac{\mathfrak{J}_2}{\mathfrak{J}_1} > 0$	$N_0(0,0)$,$N_3(r_3,0)$,$N_4\left(r_4,0\right)$; $r_{3,4} = \pm\sqrt{\frac{-\mathfrak{J}_3-\sqrt{\mathfrak{J}_4}}{2\mathfrak{J}_4}}$	$D_{0,0} < 0, Trace\left(M\left(N_{1,2}\right)\right) = 0, D_{3,0} > 0, D_{4,0} > 0$,, so, the N_0 saddle, and N_3,and N_4 are center points shown in Fig. 3i		Unstable at N_0, and stable $N_{3,4}$
	$-\frac{\mathfrak{J}_2}{\mathfrak{J}_1} > 0$	$N_0(0,0)$,$N_5(r_5,0)$,$N_6\left(r_6,0\right)$; $r_{5,6} = \pm\sqrt{\frac{-\mathfrak{J}_3+\sqrt{\mathfrak{J}_4}}{2\mathfrak{J}_4}}$	$D_{0,0} > 0, Trace\left(M\left(N_0\right)\right) = 0, D_{5,0} < 0, D_{6,0} < 0$, so, the N_0 center, and N_5,and N_6 are saddle points shown in Fig. 3(ii)		Stable at N_0, and Unstable $N_{5,6}$
$\mathfrak{J}_3^2 > 4\mathfrak{J}_1\mathfrak{J}_4 > 0$, $\mathfrak{J}_3\mathfrak{J}_4 < 0$, and $-\frac{\mathfrak{J}_2}{\mathfrak{J}_1} > 0$	$\mathfrak{J}_3^2 = \frac{16}{3}\mathfrak{J}_2\mathfrak{J}_4$,	$N_0(0,0)$,$N_3(r_3,0)$,$N_4\left(r_4,0\right)$, $N_5(r_5,0)$,$N_6\left(r_6,0\right)$	$D_{0,0} < 0$,$D_{3,0} > 0, D_{4,0} > 0$ and $Trace$ $\left(M\left(N_{5,6}\right)\right) = 0$, So, N_0,N_5, N_6 are saddle points, N_3, N_4 are center points	$\mathcal{H}\left(N_0\right) = \mathcal{H}\left(N_{5,6}\right) > \mathcal{H}\left(N_{3,4}\right)$ .The phase portrait shown in Fig. 4i	Stable at N_3,N_4, and unstable at N_0 ,N_5,N_6
	$\mathfrak{J}_3^2 > \frac{16}{3}\mathfrak{J}_2\mathfrak{J}_4$			$\mathcal{H}\left(N_{5,6}\right) > \mathcal{H}\left(N_0\right) > \mathcal{H}\left(N_{3,4}\right)$. The phase portrait shown in Fig. 4(ii)	
	$\mathfrak{J}_3^2 < \frac{16}{3}\mathfrak{J}_2\mathfrak{J}_4$			$\mathcal{H}\left(N_0\right) > \mathcal{H}\left(N_{5,6}\right) > \mathcal{H}\left(N_{3,4}\right)$. The phase portrait shown in Fig. 4(iii)	
$\mathfrak{J}_3^2 \geq 4\mathfrak{J}_1\mathfrak{J}_4 > 0, \mathfrak{J}_3\mathfrak{J}_4 < 0$, and $-\frac{\mathfrak{J}_2}{\mathfrak{J}_1} < 0$		$N_0(0,0)$,$N_3(r_3,0)$,$N_4\left(r_4,0\right)$, $N_5(r_5,0)$,$N_6\left(r_6,0\right)$	$D_{3,0} < 0, D_{4,0} < 0, J\left(N_{0,5,6}\right) > 0$ and $Trace$ $\left(M\left(N_{0,5,6}\right)\right) = 0$, So, N_0,N_5, N_6 are center points, N_3, N_4 are saddle points shown in Fig. 4(iv)		Unstable at N_3,N_4, and stable at N_0 ,N_5,N_6

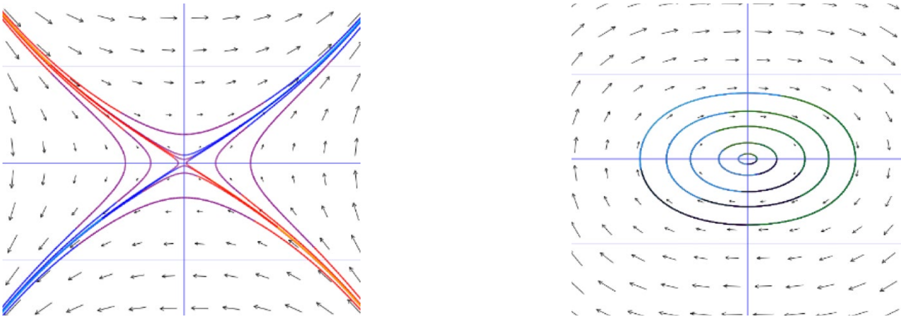

(i) (ii)

Fig. 1 Profile of the phase portrait of Event 1

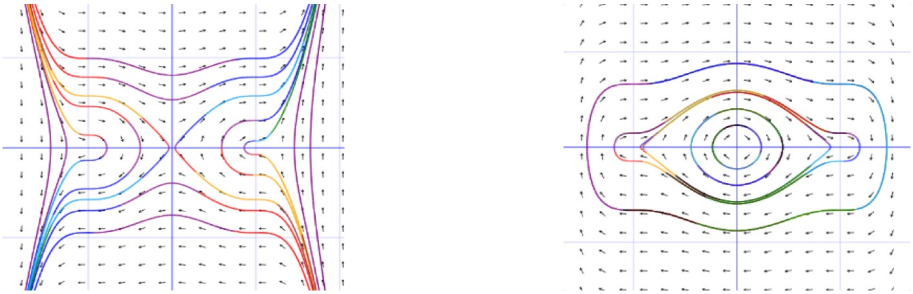

(i) (ii)

Fig. 2 Profile of the phase portrait of Event 2

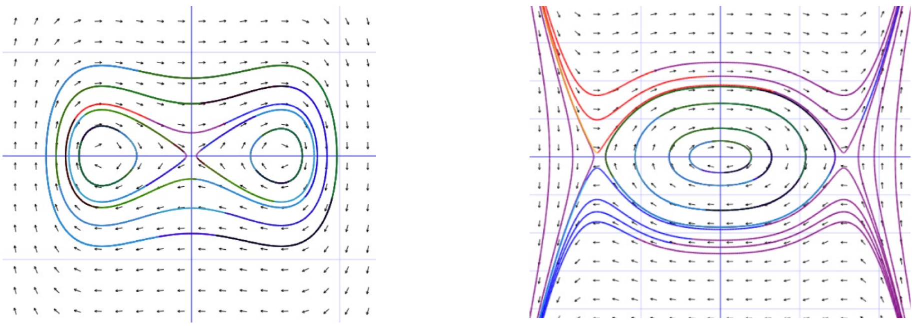

(i) (ii)

Fig. 3 Profile of the phase portrait of subevent 3

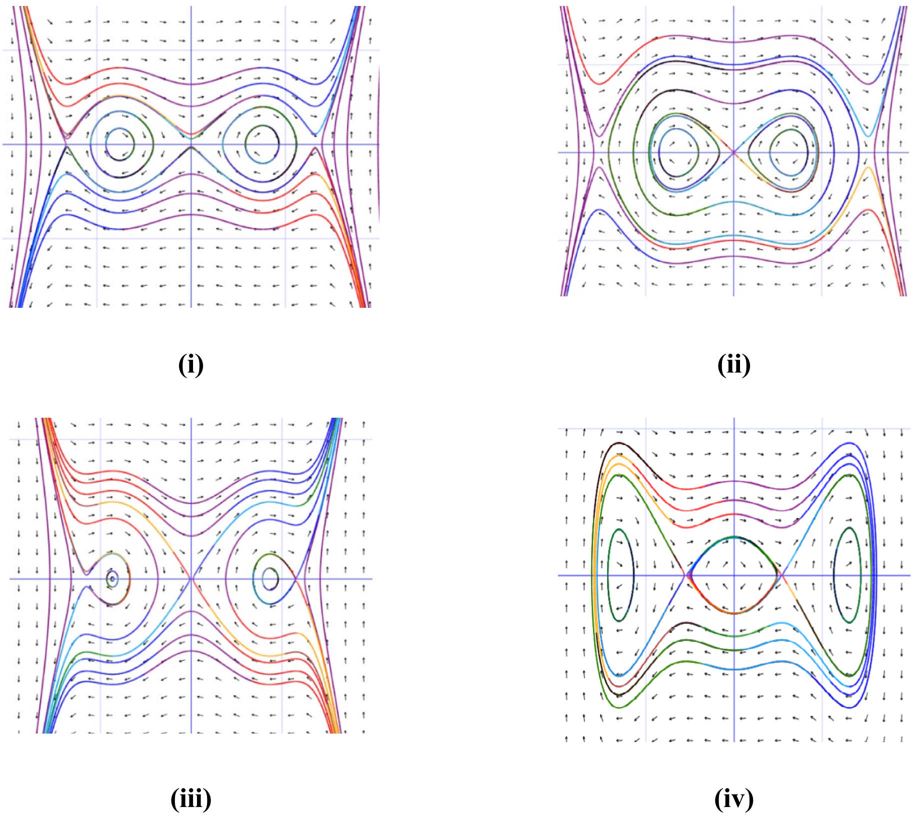

Fig. 4 Profile of the phase portrait of subevent 4

Lemma 4.1. (see Ref. [31]) Consider a coefficient matrix as:

$$M(\mathfrak{U}_0, \mathcal{L}_0) = \begin{bmatrix} 0 & 1 \\ -\frac{\mathfrak{I}_2}{\mathfrak{I}_1} & 0 \end{bmatrix}$$

The Jacobian matrix of (8) is presented as follows:

$$J(\mathfrak{U}_i, \mathcal{L}_j) = \begin{bmatrix} 0 & 1 \\ -\frac{5\mathfrak{I}_4}{\mathfrak{I}_1}\mathfrak{U}_i^4 - \frac{3\mathfrak{I}_3}{\mathfrak{I}_1}\mathfrak{U}_i^2 - \frac{\mathfrak{I}_2}{\mathfrak{I}_1} & 0 \end{bmatrix}$$

$$\Rightarrow D_{i,j} = \left|J(\mathfrak{U}_i, \mathcal{L}_j)\right| = \frac{5\mathfrak{I}_4}{\mathfrak{I}_1}\mathfrak{U}_i^4 + \frac{3\mathfrak{I}_3}{\mathfrak{I}_1}\mathfrak{U}_i^2 + \frac{\mathfrak{I}_2}{\mathfrak{I}_1}$$

Here, we defined the behaviors of the EP $(\mathfrak{U}_i, \mathcal{L}_j)$ according to $D_{i,j}$.

- If $D_{i,j} < 0$, then it is referred to as a saddle point, indicating that the system is unstable.
- If $D_{i,j} > 0$, then it is referred to as a center point, indicating that the system is stable.
- If $D_{i,j} = 0$, then it is referred to as a cusp point, indicating that the system is unstable.

- If $Trace\left(M\left(\mathfrak{U}_0, \mathcal{L}_0\right)\right) = 0$, and $D_{i,j} > 0$, then it is referred to as a node point, indicating that the system is unstable.

Lemma 2.2. (see Ref. [31]). The solution of the system (8) depends on the limiting values of the function $\mathfrak{U}(\Xi)$, and $\Xi \in (-\infty, +\infty)$. For $\lim\limits_{\Xi\to+\infty} \mathfrak{U}(\Xi) = \lim\limits_{\Xi\to-\infty} \mathfrak{U}(\Xi)$, the solitary wave and homoclinic orbit exist for the system (8). For $\lim\limits_{\Xi\to+\infty} \mathfrak{U}(\Xi) \neq \lim\limits_{\Xi\to-\infty} \mathfrak{U}(\Xi)$, the kink/bell wave and heteroclinic orbit exist for the system (8).

3 Construction of Soliton Solution for the Proposed Model

This section presents soliton solutions by integrating the homoclinic and heteroclinic orbits. In this framework, we investigate the traveling wave solutions for Eq. (4) corresponding to event-03 and event-04. Similarly, we integrate the other cases. The energy curve is defined as:

$$\} \in \mathbb{R}, C_{\}} = (\mathfrak{U}, \mathcal{L}) \in \mathbb{R} \times \mathbb{R} : H(\mathfrak{U}, \mathcal{L}) = h$$

Here h is the level of energy. Now the relation of energy level and bound orbits is as follows:

$$\mathcal{F}_h(\mathfrak{U}) = \frac{\mathfrak{F}_4}{6\mathfrak{F}_1}\mathfrak{U}^6 + \frac{\mathfrak{F}_2}{2\mathfrak{F}_1}\mathfrak{U}^2 + \frac{\mathfrak{F}_3}{4\mathfrak{F}_1}\mathfrak{U}^4 + h$$

Here the curve $f_h(\mathfrak{U}, \mathcal{L}) = \frac{\mathcal{L}^2}{2}$ also the same as the energy curve C_h and also define as $h_1 = -\mathcal{F}_1\left(N_{3,4}\right), h_2 = -\mathcal{F}_2\left(N_{5,6}\right)$.

Based on the aforementioned assumption, traveling-wave solutions are obtained for Eq. (4). The subsequent subsection examines wave propagation as described in Eq. (4).

3.1 For $\mathfrak{F}_2\mathfrak{F}_3 < 0, -\frac{\mathfrak{F}_2}{\mathfrak{F}_1} > 0$, the periodic, solitary wave solutions are illustrated under the conditions $\mathfrak{F}_2\mathfrak{F}_3 < 0, -\frac{\mathfrak{F}_2}{\mathfrak{F}_1} > 0$, and $h_1 < 0$.

For $h = 0$, a proportionate homoclinic orbit intersects at N_0 and the function $f_h(\mathfrak{U}, \mathcal{L}) = \frac{\mathcal{L}^2}{2}$ and $\mathcal{F}_h(\mathfrak{U}) = \frac{\mathfrak{F}_4}{6\mathfrak{F}_1}\mathfrak{U}^6 + \frac{\mathfrak{F}_2}{2\mathfrak{F}_1}\mathfrak{U}^2 + \frac{\mathfrak{F}_3}{4\mathfrak{F}_1}\mathfrak{U}^4 + h$ demarcated in $(\mathfrak{U}, \mathcal{L})$ – plane as:

$$\mathcal{L} = \pm\sqrt{\frac{\mathfrak{F}_4}{3\mathfrak{F}_1}\mathfrak{U}^2(\mathfrak{A}_1 - \mathfrak{U}^2)(\mathfrak{A}_2 - \mathfrak{U}^2)} \tag{11}$$

where $\mathfrak{A}_{1,2} = \frac{\pm\sqrt{9\mathfrak{F}_3^2 - 48\mathfrak{F}_2\mathfrak{F}_4 - 3\mathfrak{F}_3}}{4\mathfrak{F}_4}, \mathfrak{A}_1 > 0 > \mathfrak{A}_2$,

From Eq. (9) and the first Eq. (8),

$$\frac{d\mathfrak{U}}{d\Xi} = \pm\sqrt{\frac{\mathfrak{F}_4}{3\mathfrak{F}_1}\mathfrak{U}^2(\mathfrak{A}_1 - \mathfrak{U}^2)(\mathfrak{A}_2 - \mathfrak{U}^2)}$$

After integrating, we get the following solution:

$$\mathfrak{U}_1(\Xi) = \pm\left[\frac{\mathfrak{A}_1\mathfrak{A}_2 sech^2\left(\Xi\sqrt{-\frac{\mathfrak{I}_4}{3\mathfrak{I}_1}\mathfrak{A}_1\mathfrak{A}_2}\right)}{\mathfrak{A}_2 - \mathfrak{A}_1 tanh^2\left(\Xi\sqrt{-\frac{\mathfrak{I}_4}{3\mathfrak{I}_1}\mathfrak{A}_1\mathfrak{A}_2}\right)}\right]^{\frac{1}{2}}$$

Then the orbit represents the solitary wave solutions as:

$$L_{1\pm} = \pm\left[\frac{\mathfrak{A}_1\mathfrak{A}_2 sech^2\left(\left(\Updownarrow x - \backslash t\right)\sqrt{-\frac{\mathfrak{I}_4}{3\mathfrak{I}_1}\mathfrak{A}_1\mathfrak{A}_2}\right)}{\mathfrak{A}_2 - \mathfrak{A}_1 tanh^2\left(\left(\Updownarrow x - \backslash t\right)\sqrt{-\frac{\mathfrak{I}_4}{3\mathfrak{I}_1}\mathfrak{A}_1\mathfrak{A}_2}\right)}\right]^{\frac{1}{2}} \tag{12}$$

For the parameters $\mathfrak{I}_1 = \frac{1}{3}, \mathfrak{I}_2 = -1, \mathfrak{I}_3 = \frac{1}{3}, \mathfrak{I}_4 = 1$, $\Updownarrow = \backslash = 1$, the obtained solution, Eq. (10) has the following form:

$$\left|L_{1\pm}\right| = \pm\left[\frac{3sech^2\left(\sqrt{3}(x-t)\right)}{2 - \frac{3}{2}tanh^2\left(\sqrt{3}(x-t)\right)}\right]^{\frac{1}{2}} \tag{13}$$

For the parameters $\mathfrak{I}_1 = \frac{1}{3}, \mathfrak{I}_2 = -1, \mathfrak{I}_3 = \frac{1}{3}, \mathfrak{I}_4 = 1$, $m = n = 1$, the solution form $\left|\mathfrak{U}_1\right|$, and $\left|L_{1\pm}\right|$ is same and presents the solitary wave solution shown in Fig. 5.

2. For $h \in (h_1, 0)$, subsequently, we observe that the homoclinic orbit possesses two center points, N_3 and N_4, which are encircled by two families of periodic orbits, and it is delineated on the $(\mathfrak{U}, \mathcal{L})$-Plane as:

$$\mathcal{L} = \pm\sqrt{\frac{\mathfrak{I}_4}{3\mathfrak{I}_1}(\mathfrak{B}_1 - \mathfrak{U}^2)(\mathfrak{U}^2 - \mathfrak{B}_2)(\mathfrak{B}_3 - \mathfrak{U}^2)} \tag{14}$$

where $0 < \mathfrak{B}_1 < N_{3,4}^2$, $\widetilde{\mathfrak{B}} = \mathfrak{B}_1 + \frac{3\mathcal{J}_3}{2\mathcal{J}_4}$, $\mathfrak{B}_3 > \mathfrak{B}_1 > 0 > \mathfrak{B}_2$, $\mathfrak{B}_{2,3} = \frac{\pm\sqrt{\widetilde{\mathfrak{B}}^2 - 4\left(\widetilde{\mathfrak{B}}\mathfrak{B}_1 + \frac{3\mathcal{J}_2}{\mathcal{J}_4}\right)} - \widetilde{\mathfrak{B}}}{2}$

From the Eq. (12) and the first equation of Eq. (8), we get the following periodic solution:

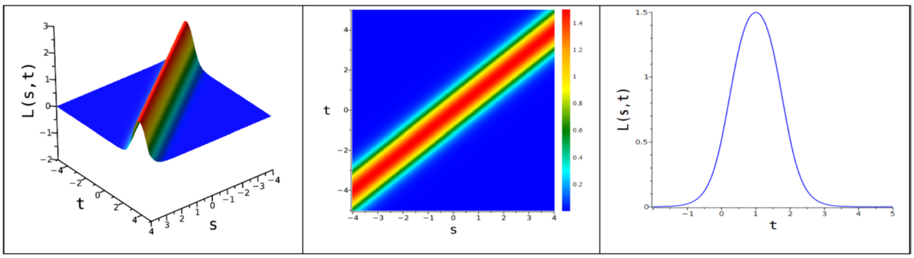

Fig. 5 Physical nature of $\left|L_1\right|$

$$\mathfrak{U}_2 = \left[\frac{\mathfrak{I}_1 \mathfrak{I}_3}{\mathfrak{B}_3 + \left(\mathfrak{B}_3 - \mathfrak{B}_1\right) cn^2(\Xi \mathfrak{C}_2, K_2)} \right]^{\frac{1}{2}} \tag{15}$$

This is a Jacobi solution and enclosed the critical points N_1, and N_2 and the parameters $\mathfrak{C}_2 = \pm\sqrt{\frac{\mathfrak{I}_4}{3\mathfrak{I}_1}\mathfrak{B}_3\left(\mathfrak{B}_1 - \mathfrak{B}_2\right)}, K_2 = \sqrt{\frac{\mathfrak{B}_2(\mathfrak{B}_1 - \mathfrak{B}_3)}{\mathfrak{B}_3(\mathfrak{B}_1 - \mathfrak{B}_2)}}$.

Then the orbit represents the solitary wave solutions as:

$$L_{2\pm} = \pm \left[\frac{\mathfrak{I}_1 \mathfrak{I}_3}{\mathfrak{B}_3 + \left(\mathfrak{B}_3 - \mathfrak{B}_1\right) cn^2((\Updownarrow x - \backslash t)\mathfrak{C}_2, K_2)} \right]^{\frac{1}{2}} \tag{16}$$

Equation (14) represents the periodic wave solution. For $\mathfrak{I}_1 = -1, \mathfrak{I}_2 = 1, \mathfrak{I}_3 = 6, \mathfrak{I}_4 = -1,\ m = n = 1$, the solutions (13) and (14) same, and the illustration of the periodic solutions of $\mathfrak{U}_2$ and L_2 in Fig. 6.

3. If $h > 0$, then, we see that three equilibrium points, $N_0, N_{3,4}$, are surrounded by an aperiodic orbit. When $\mathfrak{F}_1 < \mathfrak{F}_1 < \mathfrak{F}_2$, The answers for periodic waves can be written as:

$$L_{3\pm} = \pm \left[\frac{\mathfrak{F}_2 \mathfrak{F}_3}{\mathfrak{F}_2 + \left(\mathfrak{F}_3 - \mathfrak{F}_2\right) cn^2(\mathfrak{C}_3(\Updownarrow x - \backslash t), K_3)} \right]^{\frac{1}{2}} \tag{17}$$

where $\mathfrak{C}_3 = \pm\sqrt{\frac{\mathfrak{I}_4 B_2}{3\mathfrak{I}_1}(-\mathfrak{F}_1 + \mathfrak{F}_3)}, \mathfrak{F}_{2,3} = \frac{-\widetilde{\mathfrak{F}} \pm \sqrt{\widetilde{\mathfrak{F}}^2 - 4\left(\widetilde{\mathfrak{F}}\mathfrak{F}_1 + \frac{3\mathfrak{I}_2}{\mathfrak{I}_4}\right)}}{2}, K_3 = \sqrt{\frac{\mathfrak{F}_1(-\mathfrak{F}_2 + \mathfrak{F}_3)}{\mathfrak{F}_2(-\mathfrak{F}_1 + \mathfrak{F}_3)}}$,$\widetilde{\mathfrak{F}} = \mathfrak{F}_1 + \frac{3\mathcal{J}_3}{2\mathcal{J}_4}, \mathfrak{F}_2 < \mathfrak{F}_3 < 0 < \mathfrak{F}_1$.

For $\mathfrak{I}_1 = \frac{1}{3}, \mathfrak{I}_2 = -1, \mathfrak{I}_3 = \frac{1}{3}, \mathfrak{I}_4 = 1,\ m = n = 1$, the nature of the periodic wave of Eq. (15) is illustrated in Fig. 7.

If $\mathfrak{F}_1 > \rho_2$, the nature of periodic wave can be expressed by:

$$|L_{4\pm}| = \pm \left[\frac{\mathfrak{F}_1 \sqrt{B_5} cn\left(2\mathfrak{C}_4(\Updownarrow x - \backslash t), k_4\right) + \mathfrak{F}_1 \sqrt{\mathfrak{F}_5}}{\mathcal{O}_1 + \mathcal{O}_2 cn\left(2\mathfrak{C}_4(\Updownarrow x - \backslash t), K_4\right)} \right]^{\frac{1}{2}} \tag{18}$$

where $\mathfrak{F}_4 = \frac{3\mathfrak{I}_3}{2\mathfrak{I}_4} + \mathfrak{F}_1, \mathfrak{F}_5 = \mathfrak{F}_1^2 + \frac{3\mathfrak{I}_2}{\mathfrak{I}_4} + \frac{3\mathfrak{I}_3}{2\mathfrak{I}_4}\mathfrak{F}_1,\quad \mathfrak{C}_4 = \pm\sqrt{\frac{\mathfrak{I}_4}{3\mathfrak{I}_1}}\left[\mathfrak{F}_5(\mathfrak{F}_1^2 + \mathfrak{F}_5 + \mathfrak{F}_4\mathfrak{F}_1)\right]^{\frac{1}{4}}$, $K_4 = \frac{\left[2 - \frac{2\mathfrak{F}_5 + \mathfrak{F}_4\mathfrak{F}_1}{\sqrt{\mathfrak{F}_5\left(\mathfrak{F}_1^2 + \mathfrak{F}_5 + \mathfrak{F}_4\mathfrak{F}_1\right)}}\right]^{\frac{1}{2}}}{2}, \mathcal{O}_{1,2} = \sqrt{\mathfrak{F}^5} \pm \sqrt{\mathfrak{F}_1^2 + \mathfrak{F}_5 + \mathfrak{F}_4\mathfrak{F}_1}$.

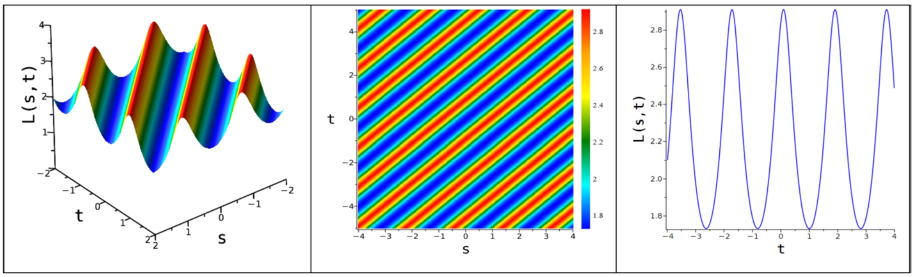

Fig. 6 Physical nature of L_2

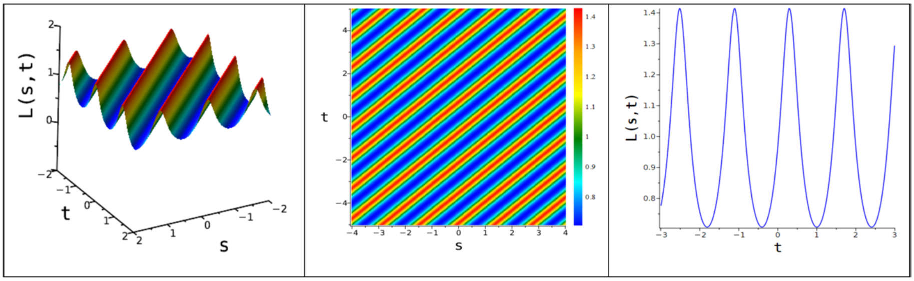

Fig. 7 Physical nature of L_3

For $\mathfrak{I}_1 = \frac{1}{3}, \mathfrak{I}_2 = -1, \mathfrak{I}_3 = \frac{1}{3}, \mathfrak{I}_4 = 1,\ m = n = 1,$ then the solution Eq. (16) presented the nature of periodic wave solution shown in Fig. 8.

3.2 When $\mathfrak{I}_2\mathfrak{I}_4 < 0, -\frac{\mathfrak{I}_2}{\mathfrak{I}_1} < 0$

For $\mathfrak{I}_1\mathfrak{I}_2 < 0, -\frac{\mathfrak{I}_2}{v_1} < 0, h_2 > 0$ the solitary waves are discussed. When $h = h_2$ We note that two symmetric heteroclinic orbits overlap at the saddle points.

$N_{5,6}$ and defined in $(\mathfrak{U}, \mathcal{L})$-plane, the expressions of the heteroclinic orbits are given as:

$$\mathcal{L} = \pm\sqrt{-\frac{\mathfrak{I}_4}{3\mathfrak{I}_1}\left(\mathfrak{I}_1 - \mathfrak{U}^2\right)^2(\mathfrak{I}_2 - \mathfrak{U}^2)} \tag{19}$$

where $\mathfrak{I}_1 = \frac{-\mathcal{J}_3+\sqrt{\Delta}}{2\mathcal{J}_4}, \mathfrak{I}_2 = \frac{-\mathcal{J}_3-2\sqrt{\Delta}}{2\mathcal{J}_4}, \mathfrak{I}_1 > 0 > \mathfrak{I}_2.$

From the Eq. (17) and the first Eq. (8), we get the following solution:

$$L_{5\pm} = \pm\left[\frac{-\mathfrak{I}_1\mathfrak{I}_2 tanh^2\left((\Updownarrow x - \backslash t)\sqrt{-\frac{\mathfrak{I}_4}{3\mathfrak{I}_1}(\mathfrak{I}_1 - \mathfrak{I}_2)}\right)}{\mathfrak{I}_1 sech^2\left((\Updownarrow x - \backslash t)\sqrt{-\frac{\mathfrak{I}_4}{3\mathfrak{I}_1}\rho_1(\mathfrak{I}_1 - \mathfrak{I}_2)}\right) - \mathfrak{I}_2}\right]^{\frac{1}{2}} \tag{20}$$

For $\mathfrak{I}_1 = -1, \mathfrak{I}_2 = -\frac{1}{4}, \mathfrak{I}_3 = 1, \mathfrak{I}_4 = 3,\ m = n = 1,$ the solution Eq. (18) presented the nature of solitary wave in Eq. (18) is shown in Fig. 9.

When $h \in (0, h_2)$, There is a periodic orbit that surrounds a center pointN_0, which is inside the heteroclinic orbits, defined in $(\mathfrak{U}, L)$-plane as:

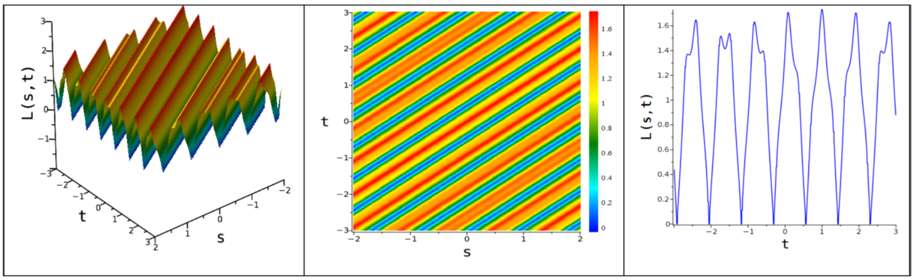

Fig. 8 Physical nature of L_4

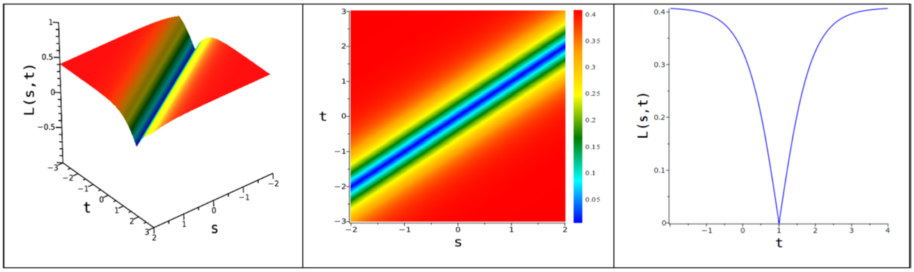

Fig. 9 Physical nature of L_5

$$\mathcal{L} = \pm\sqrt{-\frac{\mathfrak{I}_4}{3\mathfrak{I}_1}(\mathfrak{U}^2 - \mathfrak{K}_2)\left(\mathfrak{K}_1 - \mathfrak{U}^2\right)(\mathfrak{U}^2 - \mathfrak{K}_3)} \tag{21}$$

where,$0 < \mathfrak{K}_2 < \mathfrak{I}_1 \widetilde{\mathfrak{K}} = \frac{3\mathcal{J}_3}{2\mathcal{J}_4} + \mathfrak{K}_1$,$\mathfrak{K}_3 > \mathfrak{K}_1 > 0 > \mathfrak{K}_2, \mathfrak{K}_{2,3} = \frac{-\widetilde{\mathfrak{K}}\pm\sqrt{\widetilde{\mathfrak{K}}^2-4\left(\widetilde{\mathfrak{K}}\mathfrak{K}_1+\frac{3\mathcal{J}_2}{\mathcal{J}_4}\right)}}{2}$.

From the Eq. (19) and the first Eq. (8), we get the following solution:

$$\left|L_{6\pm}\right| = \pm\left[\frac{-\mathfrak{K}_1\mathfrak{K}_2 sn^2\left(L_1(\Updownarrow x - \backslash t), K_1\right)}{\mathfrak{K}_1 cn^2\left(\mathfrak{C}_1(\Updownarrow x - \backslash t), K_1\right) - q_2}\right]^{\frac{1}{2}} \tag{22}$$

where $\mathfrak{C}_1 = \pm\sqrt{-\frac{\mathfrak{I}_4}{3\mathfrak{I}_1}\mathfrak{K}_3(\mathfrak{K}_1 - \mathfrak{K}_2)}$,$K_1 = \pm\sqrt{\mathfrak{K}_1(\mathfrak{K}_3 - \mathfrak{K}_2)/\mathfrak{K}_3(\mathfrak{K}_1 - \mathfrak{K}_2)}$.

For $\mathfrak{I}_1 = -\frac{7}{3}, \mathfrak{I}_2 = -\frac{25}{12}, \mathfrak{I}_3 = 4, \mathfrak{I}_4 = 7,\ m = n = 1$, then the solution (20) represents the nature of periodic wave in Eq. (20) is shown in Fig. 10.

3.3 For$\mathfrak{I}_3^2 = \frac{16}{3}\mathfrak{I}_2\mathfrak{I}_4 > 0, -\frac{\mathfrak{I}_2}{\mathfrak{I}_1} > 0, \mathfrak{I}_3\mathfrak{I}_4 < 0$.

(1) If $h = h_2 = 0$, the heteroclinic orbits interconnect at saddle points $N_0, N_{5,6}$ and defined in $(\mathfrak{U}, \mathcal{L})$-plane as:

$$\mathcal{L} = \pm\sqrt{-\frac{\mathfrak{I}_4}{3\mathfrak{I}_1}\mathfrak{U}^2\left(\mathfrak{U}^2 - \frac{3\mathfrak{I}_3}{4\mathfrak{I}_4}\right)^2} \tag{23}$$

From Eq. (21) and the first Eq. (8), we get the kink-type wave solution by integrating this substitution.

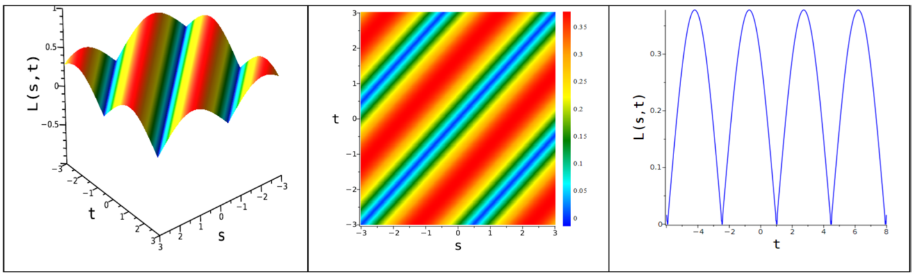

Fig. 10 Physical nature of L_6

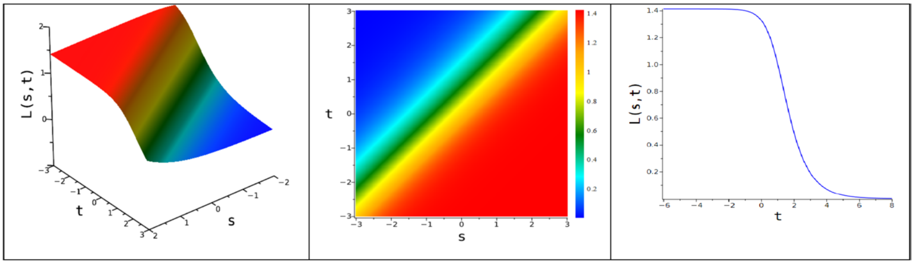

Fig. 11 Physical nature of L_{7+}

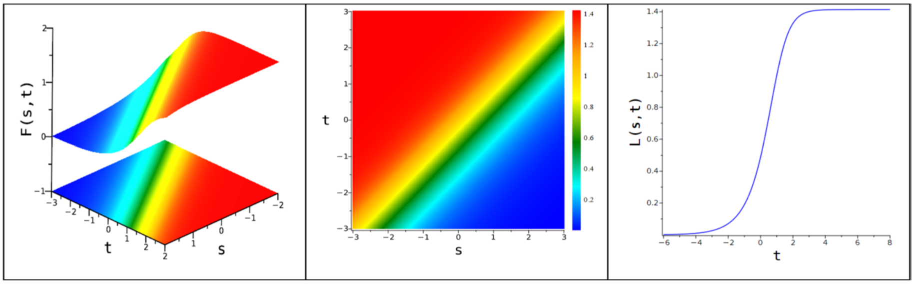

Fig. 12 Physical nature of L_{7-}

$$|L_{7\pm}| = \pm\left[-\frac{3\mathfrak{I}_3}{8\mathfrak{I}_4}\left(1 \pm tanh\left(\left(\Updownarrow x - \backslash t\right)\sqrt{-\frac{\mathfrak{I}_2}{2\mathfrak{I}_1}}\right)\right)\right]^{\frac{1}{2}} \tag{24}$$

For $\mathfrak{I}_1 = \frac{1}{3}, \mathfrak{I}_2 = -1, \mathfrak{I}_3 = \frac{1}{3}, \mathfrak{I}_4 = 1, m = n = 1$, the solution (22) represents the nature of kink wave and anti-kink wave in Fig. 11, Fig. 12 respectively.

(2) If $(h_1, 0)$, the equilibrium points $N_{3,4}$ are inside into homoclinic orbits, and surrounded by two families of periodic orbits. The periodic wave can therefore be written as:

$$|L_{8\pm}| = \pm\left[\frac{\mathfrak{L}_1\mathfrak{L}_2}{\mathfrak{L}_1 + \left(\mathfrak{L}_2 - \mathfrak{L}_1\right)cn^2\left(\mathfrak{C}_5(\Updownarrow x - \backslash t), K_5\right)}\right]^{\frac{1}{2}} \tag{25}$$

where $\mathfrak{C}_5 = \pm\sqrt{-\frac{\mathcal{J}_4}{3\mathcal{J}_1}\mathfrak{L}_2(\mathfrak{L}_3 - \mathfrak{L}_1)}, K_5 = \pm\sqrt{\mathfrak{L}_3(\mathfrak{L}_2 - \mathfrak{L}_1)/\mathfrak{L}_2(\mathfrak{L}_3 - \mathfrak{L}_1)}$ $,\mathfrak{L}_3 > \mathfrak{L}_2 > \mathfrak{L}_1 > 0.$

Under suitable parameter conditions, the solutions $L_{8\pm}$ are equivalent to $L_{4\pm}$. We disregard the particulars as we can derive analogous results from the reasoning presented in Sub Sections. 3.4 and 3.5.

3.4 When $\mathfrak{J}_3^2 > \frac{16}{3}\mathfrak{J}_2\mathfrak{J}_4 > 0, -\frac{\mathfrak{J}_2}{\mathfrak{J}_1} > 0, \mathfrak{J}_3\mathfrak{J}_4 < 0.$

(1) If $h = 0$, At the saddle pointN_0, two symmetric homoclinic orbits intersect. The solution match those in Eq. (16).
(2) If $h = h_2$, at the saddle points N_5 and N_6, two heteroclinic orbits intersect. The answers match those in Eq. (10).
(3) If $h \in (h_1, 0)$ within the homoclinic orbits, there are two families of periodic orbits. The answers are identical to those found in Eq. (18).
(4) If $h \in (h_2, 0)$ The equilibrium points N_0, N_3 and N_4 are inside a periodic orbit. The answers match those in Eq. (20).

3.5 For $0 < 4\mathfrak{J}_2\mathfrak{J}_4 < \mathfrak{J}_3^2 < \frac{16}{3}\mathfrak{J}_2\mathfrak{J}_4, -\frac{\mathfrak{J}_2}{\mathfrak{J}_1} > 0, \mathfrak{J}_3\mathfrak{J}_4 < 0.$

(1) If $h = h_2$, then a pair of symmetric homoclinic loops converge at the saddle equilibria N_5 *and* N_6. The solutions are the same as Eq. (10).
(2) If $h \in (h_1, h_2)$, then two families of periodic trajectories lie within the homoclinic loops, and their forms coincide with the solutions given in Eq. (18).

4 Modulation Instability

In this section of the study, we examine the stability of the LGH model using linear stability analysis. Let us assume the ensuing disturbed solution of the LGH model. The steady-state solution is:

$$W = K + ru(x, t) \tag{26}$$

Here K signifies the steady-state solution related to Eq. (4). By inserting Eq. (24) in Eq. (4), we obtain the following expression:

$$ru(x,t)_{tt} + au(x,t)_{xx} + b(K + ru(x,t)) + c(K + ru(x,t))^3 + p(K + ru(x,t))^5 = 0 \tag{27}$$

Linearize,

$$u(x,t)_{tt} + au(x,t)_{xx} + bu(x,t) + 3cK^2u(x,t) + 6pK^4u(x,t) = 0 \tag{28}$$

The solution that follows is derived from the equation shown:

$$u(x,t) = e^{i(\delta x - vt)} \tag{29}$$

Here, δ is employed to represent the normalized wave number, and v pertains to the frequency related to the disturbance. Now insert Eq. () into Eq. () then we get,

$$\begin{gathered} v^2 + a\delta^2 + b + 3K^2c + 6pK^4 = 0 \\ v = \sqrt{-\left(a\delta^2 + b + 3K^2c + 6pK^4\right)} \end{gathered} \tag{30}$$

Here by introducing steady-state solution with weak disturbance and performing linear stability analysis, the conditions under which the perturbation grows or decays can be identified. If $a\delta^2 + b + 3K^2c + 6pK^4 > 0$, the perturbation frequency becomes complex and the disturbance exponentially growth. This phenomenon is known as modulation instability.

Physically, MI describes the transfer of energy from a uniform wave background to localized structures, causing the breakup of a continuous wave into a train of localized pulses. Such behavior is closely related to the formation of solitons, breathers, rogue waves, and other nonlinear coherent structures. The gain spectrum shown in Fig. 13 characterizes the growth rate of unstable perturbations and identifies the frequency bands where instability is strongest. Therefore, the modulation instability analysis not only determines the stable and unstable operating regimes of the LGH model but also explains the underlying mechanism responsible for the emergence of localized nonlinear wave patterns in nonlinear media.

5 Comparison, Limitations, and Future Scope

In this section, we study the comparison of our findings with published work and present the limitations of this study. We also present the future scope of the study and how to overcome the limitations.

Comparison:

The generalized form of the proposed model was studied by Chen [10], who applied an extended method to obtain explicit and exact solutions, including bell-shaped, solitary-wave, kink-shaped, and periodic waves.

In the present studies, we explore the system's dynamics, with a particular emphasis on bifurcation theory to elucidate shifts in the qualitative attributes of the solutions. The bifurcation analysis successfully illustrated the emergence and disappearance of equilibrium points, limit cycles, and soliton formation across a range of parameter settings. Phase portraits and Hamiltonian formulations provided a deep understanding of the model's nonlinear dynamics, clearly illustrating how parameter fluctuations influence the evolution of wave patterns. The investigation of heteroclinic and homoclinic orbits produced a wide spectrum of precise wave solutions, encompassing bright periodic waves, kink and anti-kink waves, bright and dark bell-shaped waves, and solitary waves. But many researchers investigated the soliton solutions of diverse NLEEs using different methods like unified [32], auxiliary equation and the improved F-expansion [33], new extended algebraic equation [34], Sardar sub-equation [35], generalized multivariate exponential rational integral

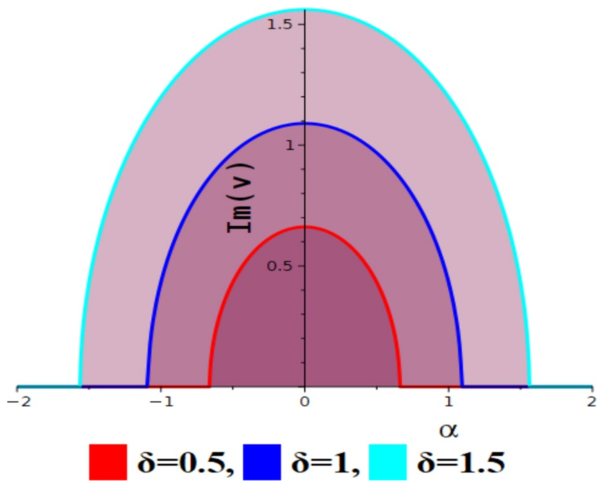

Fig. 13 Gain Spectrum of Eq. (27)

function [36] methods. Those methods solved the NLEEs with the help of auxiliary equations and takes the predefined solutions from the auxiliary equation. Otherwise, our applied method, investigated the solution directly without help of auxiliary equation or any predefined solutions. The obtained solution are explained the dynamical nature of the system.

Limitations:

The limitations of this study are:

- This work has a limitation in exploring the specific form of the GNLEEs and may not be directly applicable to all nonlinear wave models.
- The bifurcation analysis was performed only on the system's parameters, not external terms such as chaotic nature, damping effect, and external disturbance.
- The modulation instability (MI) analysis was restricted to small-amplitude perturbations and may not fully describe strongly nonlinear or turbulent wave dynamics.
- This study investigated the theoretical and computational analysis for the proposed model; experimental validation of the predicted bifurcation structures, wave solutions, and stability characteristics was not performed.

Future Scopes:

In future we investigate multidimensional iterations of the model to analyze intricate wave phenomena, such as vortices, rogue waves, and pattern generation; Analyze the interaction, collision dynamics, and long-term evolution of the derived solitary wave solutions under diverse physical conditions; Broaden the modulation instability analysis to encompass higher-order disturbances and the nonlinear phases of instability progression; Examine the effects of stochastic disturbances, external forces, and heterogeneous media on the stability and bifurcation properties of the system. Conduct an extensive parameter-space study to uncover supplementary bifurcation structures, chaotic regimes, and transition processes among various dynamical states.

6 Conclusion

This investigation provides a comprehensive analysis of the dynamical characteristics of a generalized nonlinear evolution equation (GNLEE) relevant to superconductivity, stable ion-cyclotron waves in nonhomogeneous plasma, and drift cyclotron waves. Employing both analytical and numerical approaches, the study explored the system's dynamics, with a particular emphasis on bifurcation theory to elucidate shifts in the qualitative attributes of the solutions. The bifurcation analysis successfully illustrated the genesis and disappearance of equilibrium points, limit cycles, and soliton formations across a range of parametric settings. Phase portraits and Hamiltonian formulations provided a deep comprehension of the model's nonlinear dynamics, clearly illustrating the influence of parameter fluctuations on the evolution of wave patterns. The investigation of heteroclinic and homoclinic orbits produced a wide spectrum of precise wave solutions, encompassing bright periodic waves, kink and anti-kink waves, bright and dark bell-shaped waves, and solitary waves. These solutions underscore the considerable dependence of wave morphology on the underlying nonlinear interactions and energy distributions. Thus, an analysis of modulation instability (MI) was performed to assess the amplification of small-amplitude field fluctuations. The MI findings clarify the origin of localized structures, such as solitons, domain walls, and vortices, highlighting the importance of nonlinear interactions in determining stability regions. In conclusion, the results confirm the effectiveness of the proposed analytical framework in precisely depicting complex nonlinear behaviors, thereby offering valuable insights into wave dynamics in optical, quantum, plasma, and cosmological domains.

Author Contribution M.M. Rashid: Investigation, Methodology, Writing – original draft: RM Hafez, and Y. Yildirim: Formal analysis, Software, Writing – review & editing. WX Ma: Investigation, Methodology, Writing – review & editing. All authors have read and agreed to the published version of the manuscript.

Funding No, this research did not receive funding.

Data Availability No datasets were generated or analysed during the current study.

Declarations

Ethical Approval Not applicable.

Competing interests The authors declare no competing interests.

References

1. Wazwaz, A.: Exploring multiple soliton solutions and lump wave solutions to two integrable (2+1)-dimensional Kairat-II-X-extended and Kairat-II-X-type equations. International Journal of Numerical Methods for Heat & Fluid Flow **36**(1), 145–164 (2026)
2. Farrukh, M., Alsebaey, O.N.S., Shakeel, M., Liu, X., Arshad, A., Boulaaras, S., Osman, M.S.: Bifurcation and chaos analysis with solitonic dynamics in the Kakutani–Matsuuchi model. Alexandria Engineering Journal **132**, 95–109 (2025)
3. Khalid, A., Rehan, A., Osman, M.S.: An extended third-order B-spline strategy to solve linear BVPs arising in stability analysis of electrically conducting fluid in a magnetic field. Int. J. Mod. Phys. C **33**(11), 2250153 (2022)
4. Saber, H., Roshid, M.M., Bouye, M., Muhyi, A., Moumen, A., Aldwoah, K.: Bifurcation analysis and dynamical behavior of novel optical soliton solution of chiral (2 + 1) dimensional nonlinear Schrodinger equation in telecommunication system. Sci. Rep. **15**(1), 12160 (2025)
5. Roshid, M.M., Rahman, M.M., Roshid, H.-O.: Bifurcation and modulation instability analysis, observation of closed solutions and dispersion effects on solitons in relativity and quantum mechanics. Alexandria Eng. J. **130**, 662–671 (2025)
6. Tuhin, M.H., Uddin, M., Roshid, M.M.: Data-driven estimation of optical soliton solutions with time-dependent variable coefficients for the nonlinear Schrödinger equation. J. Korean Phys. Soc. **87**(10), 1267–1280 (2025)
7. Khater, M.M.A., Alfalqi, S.H., Vokhmintsev, A.: Dynamic behavior of solitons in nonlinear Schrödinger equations. Sci. Rep. **15**, 4101 (2025)
8. Roshid, M.M., Rahman, M.M.: Bifurcation analysis, modulation instability and optical soliton solutions of the variable-coefficient nonlinear Schrödinger equation with Kerr-law nonlinearity. Nonlinear Dyn. **112**(18), 16355–16377 (2025)

9. Roshid, M.M.: Exploring chaotic behavior and ion-acoustic waves of a generalized perturbed Korteweg–de Vries equation with a fractional operator. Partial Differ. Equ. Appl. Math. **13**, 101042 (2025)
10. Chen, Y., Li, B., Zhang, H.: Exact solutions for a new class of nonlinear evolution equations with nonlinear term of any order. Chaos Solitons Fract. **17**(4), 675–682 (2003)
11. Bai, C.: Exact solutions for nonlinear partial differential equation: a new approach. Phys. Lett. A **288**, 191–195 (2001)
12. Cyrot, M.: Ginzburg–Landau theory for superconductors. Rep. Prog. Phys. **36**(2), 103–158 (1973)
13. Ablowitz, M.J., Clarkson, P.A.: Solitons, Nonlinear Evolution Equations and Inverse Scattering. Cambridge University Press, New York (1991)
14. Dodd, R.K., Eilbeck, J.C., Gibbon, J.D., Morris, H.C.: Solitons and Nonlinear Wave Equations. Academic Press, London (1982)
15. Miura, R.M.: Bäcklund Transformations. Springer, Berlin (1978)
16. Çevikel, A.C., Aksoy, E., Güner, Ö., Bekir, A.: Dark–bright soliton solutions for some evolution equations. Int. J. Nonlinear Sci. **16**(3), 195–202 (2013)
17. Iftikhar, A., Ghafoor, A., Zubair, T., Firdous, S., Mohyud-Din, T.: (G′/G, 1/G)-expansion method for traveling wave solutions of (2+1)-dimensional generalized KdV, sine-Gordon and Landau–Ginzburg–Higgs equations. Sci. Res. Essays **8**(28), 1349–1359 (2013)
18. Bekir, A., Ünsal, Ö.: Exact solutions for a class of nonlinear wave equations by using the first integral method. Int. J. Nonlinear Sci. **15**(2), 99–110 (2013)
19. Irshad, A., Mohyud-Din, S.T., Ahmed, N., Khan, U.: A new modification in the simple equation method and its applications to nonlinear equations of physical nature. Results Phys. **7**, 4232–4240 (2017)
20. Kırcı, Ö., Aktürk, T., Bulut, H.: New wave solutions in the field of superconductivity. Bitlis Eren Univ. J. Sci. **11**(2), 449–458 (2022)
21. Barman, H.K., Akbar, M.A., Osman, M.S., Nisar, K.S., Zakarya, M., Abdel-Aty, A.-H., Eleuch, H.: Solutions to the Konopelchenko–Dubrovsky equation and the Landau–Ginzburg–Higgs equation via the generalized Kudryashov technique. Results Phys. **24**, 104092 (2021)
22. Barman, H.K., Aktar, M.S., Uddin, M.H., Akbar, M.A., Baleanu, D., Osman, M.S.: Physically significant wave solutions to the Riemann wave equations and the Landau–Ginzburg–Higgs equation. Results Phys. **27**, 104517 (2021)
23. Deng, S.-X., Ge, X.-X.: Analytical solution to the local fractional Landau–Ginzburg–Higgs equation on fractal media. Thermal Sci. **25**(6), 4449–4455 (2021)
24. Roshid, M.M., Uddin, M., Abdalla, M., Ullah, M.A.: Bifurcation analysis, phase portrait and exact traveling wave propagation of an M-fractional (3+1)-dimensional nonlinear equation in a fluid medium. Opt. Quantum Electron. **57**(4), 203 (2025)
25. Algolam, M.S., Roshid, M.M., Alsharafi, M., Younis, B., Aldwoah, K., Osman, O.: Bifurcation analysis, modulation instability and dynamical analysis of soliton solutions for generalized (3 + 1)-dimensional nonlinear wave equation with m-fractional operator. Sci. Rep. **15**(1), 12929 (2025)
26. Munir, F., Saad, K.M., Abbas, M., Birhanu, A., Hamanah, W.M., Nazir, T.: Bifurcation analysis and analytical traveling wave solutions of the Sasa-Satsuma equation involving beta, M-truncated and conformable derivatives. Sci. Rep. **15**, 44483 (2025)
27. Li, Y., Shan, W.R., Shuai, T.P., Rao, K.: Bifurcation analysis and solutions of a higher-order nonlinear Schrödinger equation. Math. Probl. Eng. **2015**, 1–10 (2015)
28. Li, J., Zhang, E., Liu, M.: Bifurcation analysis and chaos control in a modified finance system with delayed feedback. Int. J. Bifurcation Chaos **26**(8), 1650132 (2016)
29. Han, T., Li, Z., Zhang, X.: Bifurcation and new exact traveling wave solutions to a time–space coupled fractional nonlinear Schrödinger equation. Phys. Lett. A **395**, 127217 (2021)
30. Du, L.X., Sun, Y.H., Wu, D.S.: Bifurcations and solutions for the generalized nonlinear Schrödinger equation. Phys. Lett. A **383**, 126028 (2019)
31. He, B., Meng, Q.: Bifurcations and new exact traveling wave solutions for the Gerdjikov-Ivanov equation. Commun. Nonlinear Sci. Numer. Simul. **15**(7), 1783–1790 (2010)
32. Akram, S., Ahmad, J.: Dynamical behaviors of analytical and localized solutions to the generalized Bogoyavlensky-Konopelchenko equation arising in mathematical physics. Optical and Quantum Electronics **56**, 380 (2024)
33. Akram, S., Ahmad, J., Turki, N.B., Shah, N.A.: On the exploration of soliton solutions of the nonlinear Manakov system and its sensitivity analysis. Results Phys. **52**, 106772 (2023)
34. Rahman, M.U., Akram, S., Baleanu, D.: Exploring new closed-form solitary waves of a nonlinear ionic transport model arising in microtubular mass flow and their global dynamical analysis. Ain Shams Eng. J. **17**(4), 104081 (2026)
35. Rahman, M.U., Akram, S.: Lump–stripe solitons and breather inelastic collision dynamics in a (3+1)-dimensional molecular-type evolution model via neural network symbolic computation. Z. Angew. Math. Phys. **77**, 93 (2026)

36. Akram, S., Taoufik, S., Rahman, M.U.: Unraveling symmetry, bifurcation dynamics, and exotic attractors analysis to the (3+1)-D modified KdV–Zakharov–Kuznetsov model. Math. Methods Appl. Sci. **49**, 2561–2584 (2026)

Authors and Affiliations

Md. Mamunur Roshid[1] · Ramy M. Hafez[2] · Yakup Yildirim[3,4] · Wen-Xiu Ma[5,6,7,8]

✉ Wen-Xiu Ma
wma3@usf.edu

✉ Md. Mamunur Roshid
mamunmath307@gmail.com

1 Department of Mathematics, Bangladesh University of Engineering and Technology (BUET), Dhaka 1000, Bangladesh

2 Department of Mathematics and Statistics, College of Science, Imam Mohammad Ibn Saud Islamic University (IMSIU), 11432 Riyadh, Saudi Arabia

3 Department of Computer Engineering, Biruni University, Istanbul 34010, Turkey

4 Mathematics Research Center, Near East University, 99138 Nicosia, Cyprus

5 Department of Mathematics, Zhejiang Normal University, Jinhua 321004, Zhejiang, China

6 Research Center of Astrophysics and Cosmology, Khazar University, 41 Mehseti Street, Baku 1096, Azerbaijan

7 Department of Mathematics and Statistics, University of South Florida, Tampa, FL 33620-5700, USA

8 Material Science Innovation and Modeling, North-West University, Mafikeng Campus, Private Bag X2046, Mmabatho 2735, South Africa